ELSEVIER

Polymer 41 (2000) 6061–6066

polymer

Application of a cycle zone-drawing/zone-annealing method to poly(ethylene terephthalate) fibers

A. Suzuki*, K. Toda, T. Kunugi

Department of Applied Chemistry and Biotechnology, Faculty of Engineering, Yamanashi University, 4-3-11 Takeda, Kofu, Yamanashi 400-8511, Japan

Received 22 February 1999; received in revised form 21 June 1999; accepted 22 November 1999

Abstract

A cycle zone-drawing/zone-annealing method was applied to poly(ethylene terephthalate) fibers in order to improve their mechanical properties. An apparatus used for this treatment was assembled in our laboratory. The cycle zone-drawing (cyZD) treatment was carried out in three steps. The first cyZD treatment was carried out at a drawing temperature of 90°C under an applied tension of 8.7 MPa, the second at 90°C under 209 MPa, and third at 130°C under 366 MPa. The number of cycles in each cyZD was 5. Subsequently, the cycle zone-annealing treatment was applied to the cycle zone-drawn fiber and carried out at an annealing temperature of 210°C under 281 MPa at the cycle number of 50. The fiber obtained finally had a birefringence of 0.255 and a degree of crystallinity of 55%. This fiber exhibited a tensile modulus of 15.1 GPa, tensile strength of 1.2 GPa, and a storage modulus of 24.3 GPa at 25°C.

Keywords: PET fiber; Cycle zone-drawing/zone-annealing; High-modulus

1. Introduction

Numerous studies have so far been carried out in the development of high-modulus and high-strength PET fibers. Fakirov et al. [1] used a two-stage cold drawing and reported a tensile modulus of 18.6 GPa and a tensile strength of 0.6 GPa. Ito et al. [2] reported that high molecular weight PET fibers, treated by using a multistep draw technique, showed a tensile modulus and strength of 39 and 2.3 GPa, respectively. We have also proposed many techniques producing high-performance fibers [3–13]. A zone-drawing/zone-annealing method is one of such treatments leading to high-modulus and high-strength fibers. The treatment was applied to PET [14] and nylon 6 [15] fibers, being revealed to be effective improvement of their mechanical properties. Further, one expected that the high performance fiber would be produced by repeating the zone-drawing and zone-annealing. These treatments were named a cycle zone-drawing (cyZD) and a cycle zone-annealing (cyZA), respectively. An apparatus used for the cyZD and cyZA was assembled in our laboratory.

It is the purpose of the present paper to improve the mechanical properties of the fiber by the cyZD and cyZA treatments. The changes in the mechanical properties and microstructure were investigated using tensile testing, dynamic viscoelasticity, thermal mechanical analysis, X-ray diffraction, density, and birefringence measurements. Further, the results of this study are compared to these of our earlier study [14] on the mechanical properties and microstructure of the ZD/ZA PET fibers.

2. Experimental

2.1. Material

The original material used in the present study was the as-spun PET fibers supplied by Toray Ltd. The original fiber had a diameter of about 0.25 mm and birefringence of 1.1×10^{-3}. The original fiber was found to be amorphous and isotropic because only an amorphous halo was observed in the wide-angle X-ray diffraction photograph as shown in Fig. 1.

2.2. Apparatus for cycle zone-drawing and cycle zone-annealing

A schematic diagram of the apparatus used for the cyZD and cyZA treatments is given in Fig. 2. The apparatus consists of a temperature-controlled zone-heater, a movable pulley, a speed control motor with equipped pulley. The looped fiber was hung on the pulley equipped with a motor and passes through the temperature-controlled

* Corresponding author. Tel.: +81-552-20-8556; fax: +81-552-20-8556.
E-mail address: a-suzuki@ab11.yamanashi.ac.jp (A. Suzuki).

0032-3861/00/$ - see front matter
PII: S0032-3861(99)00851-4

Fig. 1. Wide-angle X-ray diffraction photographs of the original fiber.

zone-heater. The movable pulley was suspended underneath the looped fiber. A tension for the fiber was arbitrarily applied by hanging a weight on the hook attached to the movable pulley. The looped fiber was rotated at constant rate by the speed control motors, drawn, and annealed up to the prescribed number of cycles.

2.3. Measurement

The draw ratio was determined in the usual way, by measuring the displacement of ink marks placed 10 mm apart on the fiber before drawing. Birefringence was measured with a polarizing microscope equipped with a Berek compensator. The X-Z quartz compensator cut from the single crystal was additionally used because the highly oriented PET fiber had higher retardation. The density (ρ) of the fiber was measured at 23°C by a flotation technique using a carbon tetrachloride and toluene mixture. The degree of crystallinity, expressed as a weight fraction (X_w), was obtained using the relation:

$$X_w = \{\rho_c(\rho - \rho_a)\}/\{\rho(\rho_c - \rho_a)\} \times 100 \quad (1)$$

where ρ_c and ρ_a are densities of crystalline and amorphous phases, respectively. In this measurement, a value of 1.455 g/cm^3 was assumed for ρ_c, and a value of 1.335 g/cm^3 was assumed for ρ_a [16]. The density of the amorphous regions was assumed to be constant, independent of the treatments.

Wide-angle X-ray diffraction data were obtained on a Rigaku diffractometer with a Ni-filtered CuK$_\alpha$ (wavelength 1.542 Å) radiation generated at 40 kV and 20 mA using scattered X-rays were measured using a scintillation counter. Orientation factors of crystallites (f_c) were evaluated by using the Wilchinsky method [17] from wide-angle X-ray diffraction patterns. Amorphous orientation factors (f_a) were calculated by the following equation [18]:

$$f_a = \frac{\Delta n - \Delta n_c^\circ f_c X_v}{\Delta n_a^\circ (1 - X_v)} \quad (2)$$

where X_v is the volume fraction crystallinity, Δn_c° an intrinsic crystallite birefringence, and Δn_c° an intrinsic amorphous birefringence. These values were taken to be 0.310 and 0.275 [19], respectively.

Wide-angle X-ray diffraction photographs for the fibers were obtained with a Rigaku X-ray flat-plate camera. The radiation used was Ni-filtered CuK$_\alpha$ generated at 36 kV and 18 mA. The sample-to-film distance was 40 mm. The fiber was exposed for 3 h to the X-ray beam from a pinhole collimator with a diameter of 0.4 mm.

Thermal shrinkage was measured with a Rigaku SS-TMA at a heating rate of 5°C/min. The samples, with a 15 mm gauge length between two jaws, were held under a tension of 5 g/cm^2, which was the minimum tension to stretch a fiber tightly.

Tensile properties were determined on a Tensilon tensile testing machine (Orientec Co. Ltd.). Tensile modulus, tensile strength, and an elongation-at-break were determined from the stress–strain curves obtained at 25°C, relative humidity of 65%. Dynamic viscoelastic properties were measured at 110 Hz on a dynamic viscoelastometer Vibron DDV-II (Orientec Co. Ltd.). A 20 mm length of monofilament was needed between two jaws. Measurements were carried out over a temperature range of 25°C to about 240°C at an interval of 5°C. The average heating rate was 2°C/min.

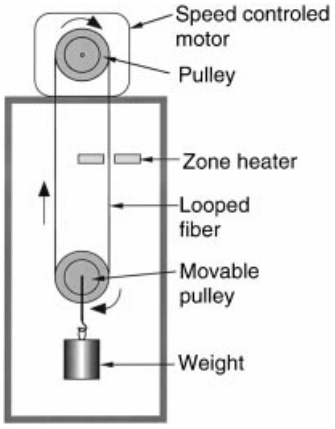

Fig. 2. Scheme of apparatus used for cyZD and cyZA.

3. Results and discussion

3.1. Optimum conditions for the cyZD and cyZA treatments

The as-spun PET fiber was drawn in three steps by the cyZD treatment, and the cycle zone-drawn fiber (cyZD fiber) was subsequently annealed under tension by the cyZA treatment. The annealed fibers were designated as cyZA fibers. The purpose of the cyZD treatment is to (as much as possible) orient amorphous chains in the drawing direction without thermal crystallization. To achieve the objective in the drawing, the cyZD treatment was carried out at the temperature range between the glass transition temperature (T_g) and the cold crystallization temperature of 130°C. Subsequently, to crystallize the amorphous chains highly oriented by the cyZD treatments, the cyZA treatment was carried out at successional higher temperatures from 180 to 220°C. To optimize the conditions for the cyZD

Table 1
Optimum conditions for the cyZD, cyZA, ZD and ZA (repetition time, ZD:1, ZA:5)

Treatment	Treating temperature (°C)	Applied tension (MPa)	Number of cycles	Treating speed (mm/min)
cyZD-1	90	8.7	5	100
cyZD-2	90	209	5	100
cyZD-3	130	366	5	100
cyZA	210	281	50	100
ZD	90	2.9	–	40
ZA	200	157	–	10

and cyZA treatments, preliminary experiments were carried out under various conditions. The optimum conditions for these treatments were determined by measuring the birefringence, the degree of crystallinity, and the storage modulus of the fibers obtained under various conditions. The resulting conditions, together with the optimum conditions for the zone-drawing (ZD) and the zone-annealing (ZA) reported previously [14], are summarized in Table 1. A maximum heating rate achieved stable drawing and annealing without whitening of a fiber was 100 mm/min. This rate was used throughout the cyZD and cyZA treatments. The microstructure and mechanical properties of the fibers obtained under optimum conditions will be discussed below.

3.2. Microstructure for the cyZD and cyZA fibers

Table 2 lists draw ratio (λ), Δn, X_w, and orientation factors of the crystallites and the amorphous regions (f_c and f_a) for the cyZD and the cyZA fibers, together with those for the ZD and ZA fibers [14]. The λ(and Δn values increase stepwise with processing, and the cyZA fiber has 6.5 and 0.255, respectively. The Δn value of the cyZA fiber is higher than that of the ZA fiber and exceeds the intrinsic crystallite birefringences ($\Delta n_c^\circ = 0.22 - 0.251$) that were reported by a number of authors [20–24]. Although the X_w value is held constant at about 30%, the Δn value increases stepwise by the cyZD treatments. The X_w increases to 30% with the cyZD-1 treatment, but increases scarcely with the subsequent cyZD treatments. Finally, the X_w value of the cyZA fiber reaches 55% which is 5% lower than that of the ZA fiber. The results suggest that the amorphous chains orient highly along the drawing direction without the additional crystallization. It is obvious from the equatorial wide angle X-ray diffraction patterns (Fig. 3) that there is no significant difference in the crystallinity between the cyZD-1 and cyZD-2 fiber.

Table 2
Draw ratio (λ), birefringence (Δn), degree of crystallinity (X_w), and orientation factors of crystallites and amorphous chains (f_c and f_a) for the original, cyZD, cyZA, ZD, and ZA fibers

Fiber	λ	Δn	X_w (%)	f_c	f_a
cyZD-1	3.8	0.194	30	0.981	0.548
cyZD-2	5.3	0.237	31	0.978	0.763
cyZD-3	6.2	0.247	33	0.988	0.802
cyZA	6.5	0.255	55	0.979	0.732
ZD	–	0.141	19	0.879	0.466 (0.412[a])
ZA	–	0.247	60	0.986	0.947 (0.605[a])

[a] The f_a values were calculated by using $\Delta n_c^\circ = 0.310$ and $\Delta n_a^\circ = 0.275$.

The f_c increases up to 0.981 with only the cyZD-1 treatment and is maintained at this high value throughout the subsequent treatments. Fig. 4 shows the wide-angle X-ray diffraction photographs of the cyZD and cyZA fibers. The azimuthal breadths of the three principal reflections, (100), ($\bar{1}10$) and (010), are sharp even in the cyZD fiber, but these spots are blurred because of its lower crystal perfection and X_w. The diffraction spots become sharper by cyZA treatment. The sharpening of the diffraction spots shows an improvement in crystal perfection and a development of the crystallinity. The f_a value increases up to 0.802 by the cyZD treatments, but decreases slightly to 0.732 by the cyZA treatment (Table 2). Although the f_a value decreases by the cyZA treatment, the orientational relaxation of amorphous chains might not occur. A small decrease in f_a reveals that the amorphous chains of relatively low orientation remain in the cyZA fiber accompanying the additional crystallization of highly oriented amorphous chains. The f_a values of the ZD and ZA fibers [14] show very high values when compared to those of the cyZD and cyZA fibers. This is because in a previous paper [14] the f_a values for the ZD and ZA fibers were estimated by using $\Delta n_c^\circ = 0.251$ and $\Delta n_a^\circ = 0.230$. The estimation of the f_a for these fibers was tried again by using $\Delta n_c^\circ = 0.310$ and $\Delta n_a^\circ = 0.275$ and then gave $f_a = 0.412$ for the ZD fiber and $f_a = 0.605$ for the ZA fiber. Therefore, the amorphous orientaitons of the cyZD and cyZA fibers are higher than those of the ZD and ZA fibers, and the amorphous chains are found to be highly oriented in the drawing direction when a fiber was treated by the cyZD and cyZA.

Fig. 5 shows the temperature dependence of thermal shrinkage for the original, cyZD, and cyZA fibers. The development of the thermal shrinkage during heating is associated with the chain coiling in the oriented amorphous regions [25]. The shrinkage depends on both the amorphous orientation and the crosslink density of the physical network formed from crystallites. The original fiber expands rapidly in the temperature range of 80–120°C and gently above 120°C. The fiber was rapidly elongated above the glass transition temperature (T_g) under a slight tension applied during the measurement. This led to strain-induced

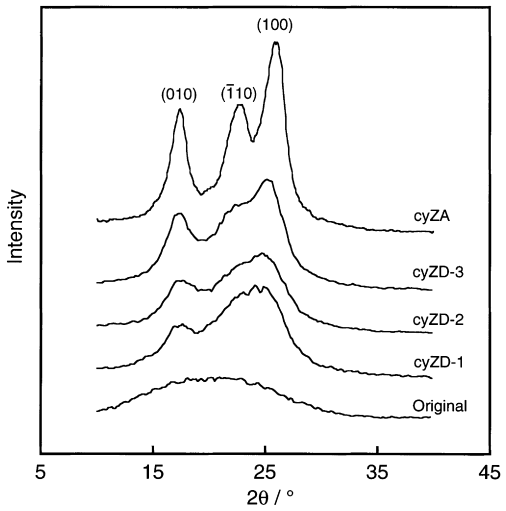

Fig. 3. Equatorial wide angle X-ray diffraction patterns of original, cyZD, and cyZA fibers.

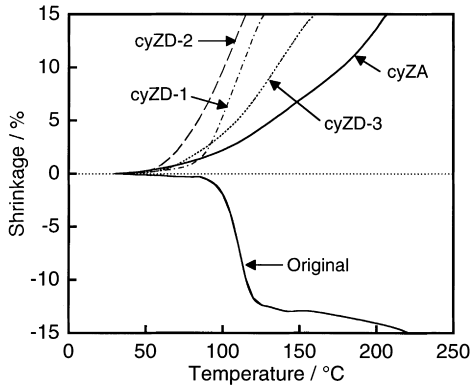

Fig. 5. Temperature dependence of thermal shrinkage the original, cyZD, and cyZA fibers.

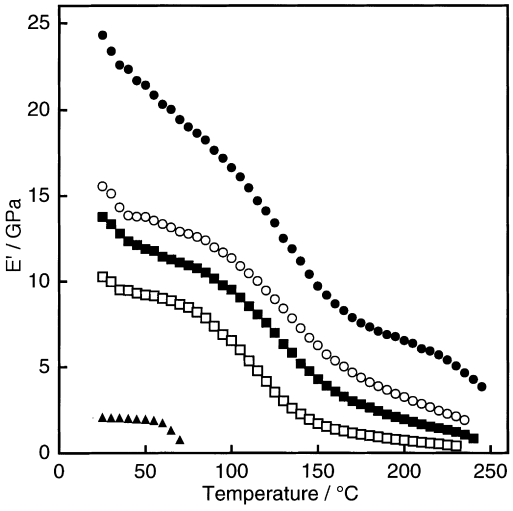

Fig. 6. Temperature dependence of storage modulus (E') for the original, cyZD, and cyZA fibers: (▲) original, (□) cyZD-1, (■) cyZD-2, (○) cyZD-3, (●) cyZA.

crystallization in the temperature range of 80–120°C. The crystallites formed act as crosslinked points to form a physical network that constrains the additional slippage of the chains. The network restricts further elongation above 120°C.

On the contrary, the cyZD and the cyZA fibers shrink above T_g as the temperature increases. The shrinkage decreases in order of treatment except the cyZD-2 treatment. We have reported the behavior of the shrinkage in the polymers obtained by various treatments. Their behavior tends to decrease stepwise with processing because both Δn and X_w increase. However, this trend does not hold good for the cyZD treatments. This is because the Δn value increases with processing, but the X_w values remain almost constant. The reversal in the shrinkage suggests that the orientation of amorphous chains in the cyZD-2 fiber is higher than that of the cyZD-1 fiber, but that the crosslink density of the cyZD-1 fiber is almost the same as that of the cyZD-2 fiber. The cyZA fiber shrinks slowly with temperature above the T_g. The difference in the behavior of the shrinkage along the cyZD and cyZA fibers is due to the difference in the crosslink density of the physical network. The physical network in the cyZD fibers was insufficient for constraint of the thermal shrinkage because of its low X_w. In the case of the cyZA fiber having a higher X_w, the oriented amorphous chains are constrained by the physical network, which has a higher crosslink density, and then chain coiling becomes increasingly difficult.

3.3. Mechanical properties for the cyZD and cyZA fibers

Table 3 lists the tensile properties of the cyZD, cyZA, ZD, and ZA fibers. The mechanical properties increase

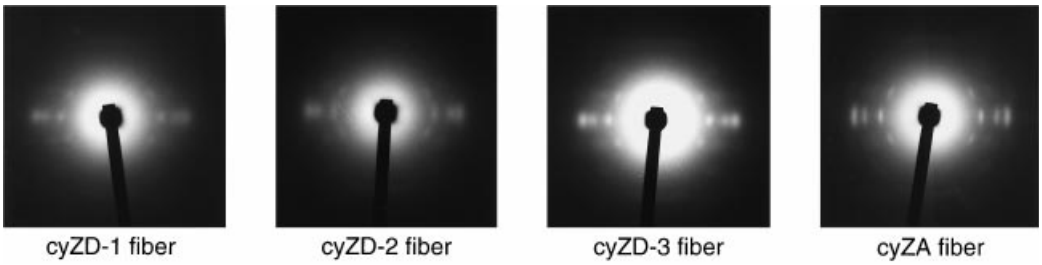

Fig. 4. Wide-angle X-ray diffraction photographs of the original, cyZD, and cyZA fibers.

Table 3
Tensile properties of the cyZD, cyZA, ZD, and ZA fibers

Fiber	Tensile modulus (GPa)	Tensile strength (GPa)	Elongation at break (%)
cZD-1	8.7	0.7	61
cyZD-2	10.6	0.8	14
cyZD-3	12.9	1.1	10
cyZA	15.1	1.2	7
ZD	6	0.1	65
ZA	19	0.8	6

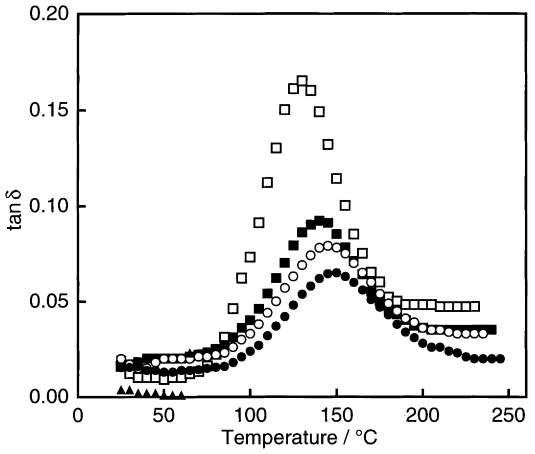

Fig. 7. Temperature dependence of tan δ for the original, cyZD, and cyZA fibers: (▲) original, (□) cyZD-1, (■) cyZD-2, (○) cyZD-3, (●) cyZA.

stepwise with increasing processing. The cyZA fiber obtained finally has a tensile modulus of 15.1 GPa and a tensile strength of 1.2 GPa. The tensile modulus of the cyZA fiber is lower than that of the ZA fiber, but the tensile strength of the cyZA fiber is higher than that of the ZA fiber.

Fig. 6 shows the temperature dependence of storage modulus (E') for the original, cyZD, and cyZA fibers. The E' values over a wide temperature range increase progressively with processing. Finally, the E' value of the cyZA fiber reaches 24.3 GPa at 25°C. The cyZA fiber is somewhat different in its viscoelastic behavior from the cyZD fibers, that is, E' of the cyZD fibers decrease more rapidly in the temperature range of 100–150°C. Viscoelastic properties of the original fiber could not be measured above the T_g because fluid-like deformation caused slippage among the amorphous chains.

Fig. 7 shows the temperature dependence of tan δ for the original, cyZD, and cyZA fibers. The cyZD and cyZA fibers show α peaks in the temperature range of 130–150°C, which are considered to originate from the glass transition. The α peak shifts to a higher temperature, decreases in its peak height, and becomes much broader with processing. The changes in position and in profile of the α peak with the processing point out that the molecular mobility in the amorphous regions is restricted by the surrounding crystallites.

4. Conclusions

The cyZD and cyZA methods have been applied to poly(ethylene terephthalate) fibers to improve their mechanical properties. The degree of crystallinity increased to 33% by the cyZD treatments, increasing up to 55% by the subsequent cyZA treatment. The orientation factor of crystallites increased from 0 to 0.981 by only the first cyZD-1 treatment. On the contrary, the amorphous orientation factor increased with processing, and the cyZD-3 fiber had 0.802. Thus, the cyZD-3 fiber shows a higher amorphous orientation and a low crystallinity. The mechanical properties rose stepwise, and the cyZA fiber obtained finally had a tensile modulus of 15 GPa, tensile strength of 1.2 GPa, and storage modulus of 24.3 GPa at 25°C. The α peak in the tan δ vs. temperature curve shifted to a higher temperature and its magnitude reduced progressively with processing.

Acknowledgements

We acknowledge the financial support of the Grant-in-Aid for Scientific Research of the Ministry of Education, Science, and Culture, Japan.

References

[1] Fakirov S, Evstaiev M. Polymer 1990;31:431.
[2] Ito M, Takahashi K, Kanamoto T. J Appl Polym Sci 1990;40:1257.
[3] Kunugi T, Suzuki A, Tsuiki T. Kobunshi Ronbunsyu 1991;48:703.
[4] Suzuki A, Maruyama S, Kunugi T. Koubunshi Ronbunsyu 1992;49:741.
[5] Suzuki A, Endo A. Polymer 1997;8:3085.
[6] Suzuki A, Murata H, Kunugi T. Polymer 1998;39:1351.
[7] Suzuki A, Sato Y, Kunugi T. J Polym Sci, Polym Phys Ed 1998;36:473.
[8] Kunugi T, Chida K, Suzuki A. J Appl Polym Sci 1998;67:1993.
[9] Suzuki A, Endo A, Kunugi T. Polym J 1998;30:275.
[10] Suzuki A, Kohno T, Kunugi T. J Polym Sci, Polym Phys Ed 1998;36:1731.
[11] Suzuki A, Kuwabara T, Kunugi T. Polymer 1998;39:4235.
[12] Suzuki A, Chen Y, Kunugi T. Polymer 1998;39:5335.
[13] Suzuki A, Endo A, Kunugi T. J Polym Sci, Polym Phys Ed 1998;36:2737.
[14] Kunugi T, Suzuki A, Hashimoto M. J Appl Polym Sci 1981;26:1951.
[15] Kunugi T, Akiyama I, Hashimoto M. Polymer 1982;23:1199.
[16] Danderg RR, Bunn CW. Proc R Soc A 1954;226:531.

[17] Wilchinsky ZW. J Appl Phys 1963;30:792.
[18] Stein RS, Norris FH. J Polym Sci 1956;21:381.
[19] Gupta VB, Sett SK, Deorukhkar DD. Polymer 1989;30:341.
[20] Patterson D, Ward IM. Trans Faraday Soc 1957;53:1516.
[21] Dumbleton JH. J Polym Sci, A-2 1968;6:795.
[22] Konda A, Nose K, Ishikawa H. J Polym Sci, A-2 1976;14:1495.
[23] Kunugi T, Shiratori K, Uematu K, Hashimoto M. Polymer 1979;20:171.
[24] Garg SK. J Appl Polym Sci 1982;27:2857.
[25] Wilson MPW. Polymer 1974;15:277.